ORIGINAL PAPER

Rapid differentiation of mafic to intermediate magma constrained by Ra–Th disequilibrium and the size of magma chamber beneath Hekla volcano, Iceland

Olgeir Sigmarsson[1,2] · Guðrún Larsen[2] · Garance Hervé[1]

Abstract

The size of deep-seated magma chambers is an important parameter for understanding pre-eruptive signals such as surface deformation. The constantly inflating Hekla volcano in Iceland has had relatively simple eruptive behaviour during the historical period. The eruptions start explosively with production of differentially evolved andesite magma to dacite, related to the length of the foregoing quiescence period, and ends with an emission of a basaltic andesite lava of uniform composition. The basaltic andesite is formed by fractional crystallisation from a deeper-seated basalt source in a steady-state manner. How fast such a differentiation mechanism operates is unknown. Measured Ra–Th radioactive disequilibrium in both the basalt and the basaltic andesite reveal a decrease from a 14% excess of ^{226}Ra over ^{230}Th to only 5% with magma differentiation. The decrease in ^{226}Ra excess to 5% in the basaltic andesite of Hekla is shown to be controlled by plagioclase fractionation alone. Therefore, the magma differentiation time from basalt to intermediate magma beneath Mt. Hekla is significantly shorter than three centuries, the time needed to detect significant ^{226}Ra-decay. Given the steady-state production of basaltic andesite magma and the estimated magma production rate, the volume of the basaltic andesite magma reservoir can be estimated as less than 2 km^3.

Keywords Rate of magma differentiation · U-series disequilibrium · ^{226}Ra–^{230}Th · Assessment of Ra solid-melt partition

Introduction

The magma plumbing system beneath a volcano needs to be better understood for improved hazard monitoring. Amongst the important parameters are the size of the active magma reservoir at depth and the magma residence time. Short-lived U-series disequilibria indicate that magma of intermediate composition can form in less than 10 years from basalt differentiation (e.g., Sigmarsson 1996). Such a short timescale for magmatic processes concurs with the increasing number of rapid trace element diffusion chronometers (e.g., Costa et al. 2020). The differentiation time of magma and the

residence time of magma reservoirs at depth have frequently been assessed through Ra–Th disequilibrium (e.g., Condomines et al. 1995, 2003; Vigier et al. 1999; Turner et al. 2003; Berlo et al. 2004; Blake and Rogers 2005; Yokoyama et al. 2006; Reagan et al. 2005; Handley et al. 2008; Chekol et al. 2011; Cooper and Kent 2014; Schlieder et al. 2022).

The relatively long half-life of ^{226}Ra ($T_{1/2}$: 1600 years), however, causes the ^{226}Ra–^{230}Th disequilibrium to be insensitive to decadal and shorter timescales. For a magma suite formed by fractional crystallisation, the decrease of the ^{226}Ra–^{230}Th disequilibrium from basalt to the more evolved magma composition will only reflect ^{226}Ra-decay if the differentiation exceeds two to three centuries. Moreover, if Ra enters the fractionating minerals, such as plagioclase, then the decreasing ^{226}Ra–^{230}Th disequilibrium can be caused entirely by melt-mineral separation and the duration of differentiation can be much shorter than inferred from radioactive decay alone. Recycling of crystals containing either Ra or Th, and of different ages also, will of course complicate the assessment of magma differentiation rates from U-series disequilibria.

Recent basaltic andesite eruptions at Hekla volcano, Iceland, allow the assessment of the ^{226}Ra–^{230}Th disequilibrium approach in estimating the timescale of magma differentiation. The constant final basaltic andesite lava composition at the end of historical eruptions at Mt. Hekla (Thorarinsson 1967; Sigmarsson et al. 1992, 2022; Chekol et al. 2011; Geist et al. 2021) suggests a basaltic andesite magma reservoir of uniform composition. The aphyric character of the basaltic andesite limits complications from recycled crystals, or disintegrated mush, and its origin from fractional crystallisation of basalt (Sigmarsson et al. 1992, 2022; Chekol et al. 2011; Geist et al. 2021) makes it an ideal case to estimate the rate of magma differentiation from a basalt to a basaltic andesite.

When magma residence time can be assessed for a magma chamber or reservoir, with a steady-state behaviour and known magma flux in and out of the reservoir, then its volume can be estimated (e.g., Pyle 1992; Condomines et al. 2003). The basaltic andesite magma reservoir beneath Hekla volcano is still undetected by seismic methods, possibly due to its small size (Soosalu and Einarsson 2004).

Hekla magma suite

During the last 1000 years, the Hekla volcanic system has produced an entire magma suite of phenocryst-poor basalt to dacite. Four eruptions of basalt are known, 1554, 1725, 1878 and 1913 CE, the two oldest erupted from craters south of Mt. Hekla whereas the two youngest came up north and east of the volcano (Fig. 1). The Lambafit 1913 CE eruption produced the most primitive basalt and has been taken as the parental magma to the basaltic andesite of Hekla proper (Sigmarsson et al. 1992; Chekol et al. 2011). The first two historical eruptions were of dacitic composition, the large explosive eruption forming the H1 tephra layer in 1104 CE and the smaller 1158 CE eruption, which formed the only silicic lava known at Hekla. Later eruptions produced tephra of basaltic andesite to evolved andesite composition with the lava being principally of basaltic andesite composition. Maximum crystallinity of basaltic andesite is 9%, which decreases with increased differentiation, and the rare phenocrysts show limited compositional zonation (Geist et al. 2021 and references therein; Supplementary Information 1). Each eruption begins explosively forming tephra but evolves through a phase of concurrent tephra-lava extrusion into a much longer lasting period of lava emission (Thorarinsson 1967). Figure 2a depicts the cumulative dense-rock-equivalent volume (DRE volume, assuming 15% vesicularity (Pedersen et al. 2018a)) of historical lava fields of Hekla. The linear cumulative volume increase with time suggests a steady-state behaviour (Wadge 1982) of the basaltic andesite magma reservoir beneath Hekla.
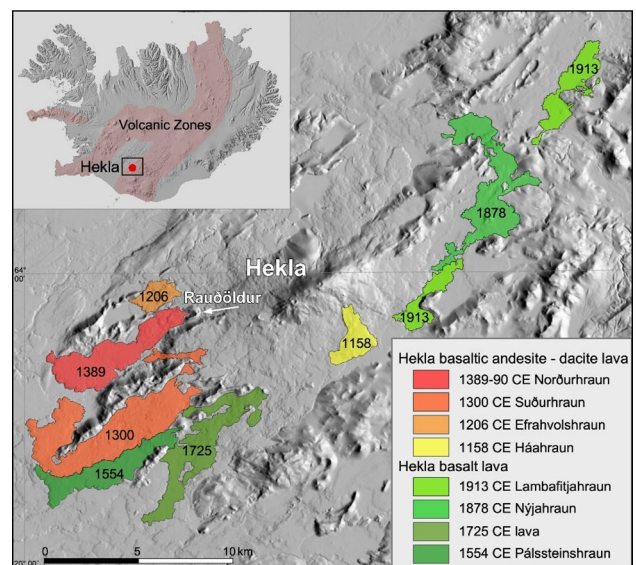
Fig. 1 Digital elevation map (DEM) of Hekla volcanic system showing the 1913 CE, 1878 CE, 1725 CE and 1554 CE basalt lava fields (green), the dacite 1158 CE Háahraun (yellow) and basaltic andesite lava from 1206 CE Efrahvolshraun, 1300 CE Suðurhraun and 1390 CE Norðurhraun (orange to red). Modified from Pedersen et al. (2018b). Younger basaltic andesite lavas cover the entire slope of Mt. Hekla (not shown). Background from ArcticDEM Explorer (Porter et al. 2023). Inset ÍslandsDEM, Landmælingar Íslands/National Land Survey of Iceland

Magma productivity at Hekla

Magma productivity, or the flux, can be estimated for the last two centuries from the measured lava and tephra volumes of the nineteenth and twentieth century eruptions. The lava volume of each of the youngest eruptions was measured from aerial photos and digital elevation maps by Pedersen et al. (2018a). Volumes for older historical lava were calculated from the mapped lava surface before the 1947–1948 CE eruption by Kjartansson (1945) and by assuming an origin at the Hekla ridge and a single average thickness for all lavas of similar composition (20 and 50 m for lavas of intermediate and silicic composition, respectively). Reassuringly, the volume estimated for the large twentieth century lava fields using the same method as for the older historical lava turn out to be within errors of the more sophisticated measurements (Pedersen et al. 2018a), which lends credit to the method used for volume estimations of older lavas. As an example, the measured volume for the 1947–1948 lava field is 0.7 ± 0.1 km^3 (Pedersen et al. 2018a) whereas the volume estimate by Thorarinsson (1967) is 0.80 km^3.

Lava volumes show a linear correlation with the lengths of repose time (Fig. 2b). Since tephra is less than 0–20% of the total volume, the correlation holds for the total volume
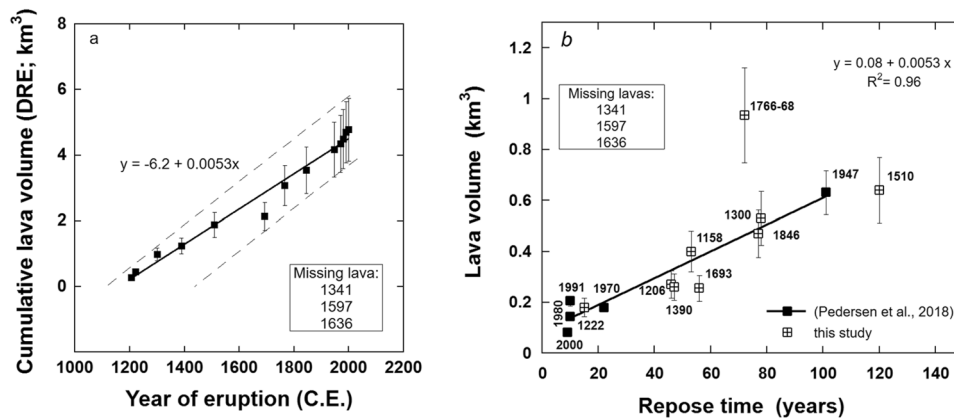
Fig. 2 a Cumulative lava volume vs. eruption year at Mt. Hekla for the historical period showing the linear increase with a production rate of 5.3×10^{-3} km^3/yr (0.2 m^3/s). The missing lava volumes from both the 1597 CE and 1636 CE eruptions explain the low value for the 1693 lava. The uniform lava production suggests that the basaltic andesite magma reservoir has a steady-state behaviour (Wadge 1982).

Lava volume as dense-rock-equivalent (DRE) with 20% assigned error. **b** Lava volumes increase linearly with the length of the repose time before the eruptions. A regression line is calculated from measured volumes of the twentieth century lava fields (Pedersen et al. 2018a), the slope of which corresponds to the long-term lava production rate of 0.0053 km^3/yr (0.2 m.^{3}/s)

produced. A linear regression coefficient is only calculated for eruption volumes of the last century, since the surface of older lavas are often partially obscured by younger lavas flowing over the older ones. The only silicic lava at Hekla, Háahraun, and the 1158 CE tephra are of identical composition, and is thus most likely from the 1158 Hekla eruption (Sigmarsson et al. 1992). Consequently, the Efrahvolshraun lava, which was thought to be from the year 1158 (Thorarinsson 1967), was most likely produced during the 1206 CE rather than the 1222 CE eruption (Sigmarsson et al. 1992; Pedersen et al. 2018b). Detailed field work (Larsen and Thordarson 2016) and information from written annals reveal that the tephra from the small 1222 CE eruption was blown to the NE. Little, or negligible, 1222 CE tephra fell on the (presumed) 16 years older, vegetation-free Efrahvolshraun lava, which explains its absence in the first cm of soil beneath the 1300 CE tephra layer on top of that very lava.

The slope of the regression line yields lava production rate of 0.0053 km^3/yr (0.20 m^3/s) with only the 1766–1768 CE lava field plotting significantly above the regression line, for unknown reasons. Several older lava fields plot below the correlation line, such as those of 1389–1390 CE and 1693 CE eruptions, possibly because the surface area was underestimated due to partial over-flowing of younger lava. Moreover, lava flows suspected to have been formed in at least three historical eruptions have not been identified yet. Extrapolation of the lava volume to repose time of nought yields 0.1 km^3, which can be considered as a minimum magma volume for an eruption at Hekla proper. Deformation measured over the decade after the 2000 Hekla eruption has been assigned to different forms of magma chambers, spherical, ellipsoidal and pipe-like forms with production

rates in the range 0.25–0.6 m^3/s by Geirsson et al. (2012) that are within error of that determined from the slope of the regression line in Fig. 2b.

Magma composition versus repose time

Since the work of Thorarinsson (1967), historical eruptive activity at Mt. Hekla is known to be a function of the length of the foregoing quiescent period, or repose time. The composition of the first emitted tephra, the vigour and length of the initial explosive phase, and the volume of magma produced are all correlated with the length of the repose time before an eruption. As for silica, the Th concentrations of the first tephra produced in each eruption strongly correlates with the repose duration. In contrast, each eruption ends with the emission of a basaltic andesite of uniform composition (SiO$_2$ ~ 54%; Th ~ 4.5 ppm). The termination with identical composition through at least the latter half of the historical period suggest that the basaltic andesite is produced in a steady-state manner.

Maximum and minimum Th concentrations are shown in Fig. 3. They are, respectively, observed in the initial tephra pumice and the final lava composition of each eruption. The squared correlation coefficient, R^2, is equal to 0.95 as calculated for all eruptions except those of 1104 CE, 1158 CE, 1206 CE and 1389 CE. The repose time before the large 1104 CE eruption is not well constrained (Thorarinsson 1967) and Óladóttir et al. (2012) argued for a duration of 250 years. Thorium concentrations of the 1104 CE tephra falls on the extrapolation of the correlation in Fig. 3 for a quiescence period of 250 years. Tephra from 1158 CE has much higher Th than expected for the 54 years elapsed since the 1104 CE. The same holds for the third historical
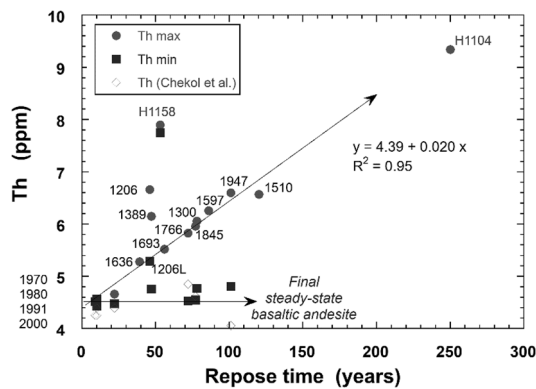
Fig. 3 Thorium concentrations in initial tephra (Th max) and lava (Th min) plotted against the length of the foregoing repose time for most historical eruptions. The regression is calculated for the first formed tephra erupted since 1300 CE, excluding that of the 1389 CE tephra. Noteworthy is the extrapolation of the regression line to the 1104 CE dacite (assuming 250 years. of quiescence before that eruption) and that the Th concentration of both the dacitic 1158 CE tephra and lava is relatively high, decreasing through the 1206 CE tephra and terminating at the 1206 CE lava. Younger lava composition is taken to represent the final steady-state magma composition of each eruption. The thorium concentrations, measured by isotope-dilution mass spectrometry, are taken from Sigmarsson et al. (1992, 2022) and Chekol et al. (2011), with a few new results given in Supplementary Information 2

eruption, namely the 1206 CE eruption. The most likely lava flow of that eruption is Efrahvolshraun, the composition of which plots on the regression line for the initial tephra composition. After that, only the tephra from the 1389 CE eruption is an outlier from the linear relationship in Fig. 3. That eruption is reported to have begun at the Hekla volcano but then relocated to a fissure some 4 km to the WSW, now marked by the large Rauðöldur scoria and spatter cone, from where the Norðurhraun lava emanated (Fig. 1; Thorarinsson 1967). The course of events is unusual, and the site of tephra emission is uncertain.

The intercept of the regression line at repose time of nought yields 4.4 ppm Th which is indistinguishable from the average concentration measured in nine lavas from the final phase of historical eruptions since 1300 CE (median 4.55 ppm; mean 4.60 ppm with 2SD of 0.28). Each eruption thus ended with lava of similar composition regardless of the length of the preceding repose time.

Samples and analytical methods

Pumice fragments with a diameter larger than 1 cm were collected at the base of historical tephra layers in soil sections close to the axis of maximum thickness (as defined by Larsen and Thordarson 2016). The Th concentrations and Th/U were analysed by isotope dilution mass spectrometry at

Laboratoire Magmas et Volcans (LMV), Clermont-Ferrand and the (^{230}Th/^{232}Th) were obtained on multi-collector ICP MS following the procedure of Carpentier et al. (2016). The twentieth century lavas, and basalt Hek-16, are an exception with average (^{230}Th/^{232}Th) taken from the abundant lava analyses of Chekol et al. (2011). The thorium isotope ratio of H1980 is a long α-spectrometer analysis from Sigmarsson et al. (1992).

Measurements of Ra activities in the magma suite of Hekla were initiated on a γ-spectrometer with two planar Ge detectors using the set-up described by Condomines et al (1995). After moving the LMV to a new location in 2015, Ra analyses were performed on a new Ge well-detector from Baltic Scientific Instruments, which allowed improved γ-ray detection and a sample size reduction down to approximately 10 gr. All Hekla samples have ^{228}Ra (measured at 338.4 keV of ^{228}Ac) in equilibrium with both ^{228}Th (measured at 238.6 keV of ^{212}Pb and 583.14 keV of ^{208}Tl) and ^{232}Th due to their age ($> 5 \times$ ^{228}Ra $T_{1/2}$, or 30 years). Most of the ^{226}Ra measurements were by isotope dilution of ^{210}Po with an artificial ^{209}Po tracer and α-spectrometry for the ^{210}Po–^{209}Po ratio. The method assumes radioactive equilibrium between ^{226}Ra and its short-lived daughter nuclides and is only applicable for rocks older, and that have remained a closed system longer, than a century (~5 times the half-life of ^{210}Pb). The absence of Ra–Pb fractionation in the twentieth century lavas is demonstrated by identical ^{226}Ra activity measured by γ-spectrometry and via ^{210}Po by α-spectrometry. Both methods yield ^{226}Ra in equilibrium with ^{230}Th measured in two obsidian standards older than 8 kyrs, namely A-THO and HSK-8. In addition, a few isotope dilution analyses of the ^{226}Ra concentrations were made on a TIMS instrument with 1% analytical uncertainty (2 SE).

The mean (^{226}Ra) in Table 1 is a weighted mean of the different Ra measurements and is used to calculate the (^{226}Ra/^{230}Th). The average two sigma relative standard deviation (2RSD) on the (^{226}Ra/^{230}Th) is 2.5% (range: 1.7–3.5%). Hereafter, only the post-eruptive decay-corrected (^{226}Ra)$_0$ will be discussed, namely the value at the time of eruption. Error propagation factor on (^{226}Ra/^{230}Th)$_0$ is very small since the exact eruption year is known and the error on the ^{226}Ra half-life is only 0.25% (Holden 1990), which is in accordance with the uncertainty propagation assessment by Pommé et al. (2014).

Results

The post-eruptional decay-corrected Ra activity (^{226}Ra)$_0$ forms an excellent linear correlation with Th concentrations for the whole magma suite (with $R^2 = 0.998$; Fig. 4) and a Y-axis intercept close to 0.1 (disintegration per min per gramme (dpm/g) of ^{226}Ra).

Table 1 Analytical results of ^{226}Ra activity in historical Hekla products

Sample	Eruption date	Rock type	Th (ppm)	(^{230}Th/^{232}Th)	2σ	(^{226}Ra) by γ-SM (dpm/g)	σ	(^{226}Ra) by (^{210}Po) (dpm/g)	σ	(^{226}Ra) by ID-TIMS (dpm/g)	(^{226}Ra) mean (dpm/g)	2σ	(^{226}Ra/^{230}Th)	2σ	(^{226}Ra/^{230}Th)$_0$	2σ
Hek-28	6500	Basalt	1.66	1.066	0.014			0.459	0.013		0.459	0.026	1.06	0.06	1	
Hek-2	7000	Basalt	1.72	1.065	0.014					0.462	0.462	0.009	1.03	0.03	1	
H1554L	1554	Basalt	3.10	1.053	0.010	0.852	0.008	0.857	0.010		0.854	0.013	1.07	0.02	1.07	0.02
H1725L	1725	Basalt	1.90	1.079	0.014			0.557	0.009		0.559	0.012	1.12	0.03	1.12	0.03
dpl		Basalt						0.561	0.008							
Hek-9	1913	Basalt	2.38	1.060	0.014	0.632	0.006	0.663	0.020	0.656	0.641	0.008	1.04	0.02	1.04	0.02
Hek-16	1913	Basalt	1.92	1.042	0.014			0.565	0.013	0.554	0.558	0.016	1.14	0.04	1.14	0.04
Hek-18	1878	Basalt	2.07	1.060	0.014	0.558	0.006	0.574	0.010		0.562	0.010	1.05	0.02	1.05	0.02
H2000	2000	Bas. and	4.52	1.017	0.009	1.172	0.011	1.166	0.016		1.170	0.018	1.04	0.02	1.04	0.02
H1991L	1991	Bas. and	4.43	1.022	0.010	1.154	0.016	1.145	0.013		1.148	0.020	1.04	0.02	1.04	0.02
H1981L	1981	Bas. and	4.58	1.018	0.013	1.198	0.012	1.184	0.017		1.193	0.020	1.05	0.02	1.05	0.02
H1980	1980	Bas. and	4.57	1.023	0.010			1.201	0.014		1.201	0.028	1.05	0.03	1.05	0.03
H1970-14	1970	Bas. and	4.48	1.023	0.009			1.183	0.017		1.183	0.034	1.06	0.03	1.06	0.03
H1846-L	1846	Bas. and	4.55	1.040	0.020	1.190	0.033	1.230	0.050		1.202	0.055	1.04	0.05	1	
H1768L	1768	Bas. and	4.53	1.040	0.012			1.214	0.020		1.214	0.040	1.06	0.04	1.06	0.04
H1693-B	1693	Andesite	5.50	1.018	0.014			1.450	0.020		1.450	0.040	1.06	0.03	1.06	0.03
H1510a	1510	Andesite	6.44	1.014	0.014			1.630	0.019		1.630	0.038	1.02	0.03	1	
H1390L	1390	Bas. and	4.76	1.021	0.010					1.18	1.180	0.024	0.99	0.02	1	
H1300L	1300	Bas. and	4.77	1.026	0.012	1.200	0.020	1.287	0.017		1.263	0.020	1.06	0.02	1.06	0.02
dpl								1.249	0.013							
Hek-8	1158	Dacite	7.75	0.987	0.014	1.905	0.016	1.950	0.025		1.918	0.027	1.03	0.02	1.03	0.02
H1104-M	1104	Dacite	9.03	0.970	0.010											
H1104-A	1104	Dacite	9.34	0.973	0.008	2.350	0.020	2.352	0.020		2.304	0.035	1.04	0.02	1.04	0.02
dpl		Dacite						2.297	0.025							

Parenthesis around nuclides denote activity. Both Th concentrations and the Th isotope ratio are from Sigmarsson et al. (1992, 2022) except). the average Th isotope ratio for Lambafit 1913 (alias Hek-16) and Hekla 1981, 1991 and 2000 lava are from Chekol et al. (2011)

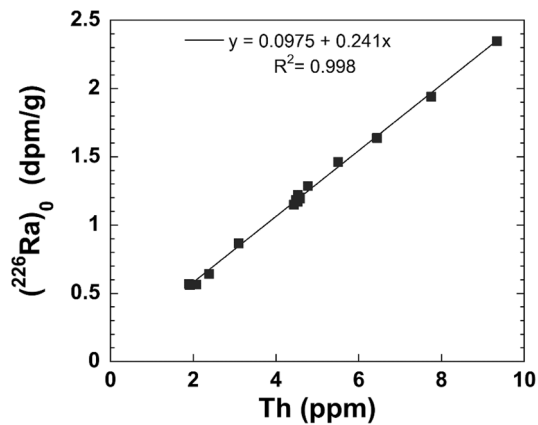*dpm* disintegration per min (dpm/g = 60 Bq/g), *dpl* duplicate measurement

Fig. 4 Activity of ^{226}Ra in disintegration per min per gramme (dpm/g = 60 Bq/g) at the time of eruption [(Ra)$_0$], in historical Hekla volcanics, plotted against Th concentrations. Intercept at the Y-axis reveals the more compatible behaviour of Ra compared to Th during fractional crystallisation of basalt forming the basaltic andesite. The magma differentiation from basaltic andesite to dacite follows the same trend, as already observed for most element concentrations (Sigmarsson et al. 1992; 2022; Geist et al. 2021). Error bars at 2σ are smaller than the symbol size

Fig. 5 Decay curve for an initial (^{226}Ra/^{230}Th) of 1.16 with time. The two hatched areas show the inaccessible ages for 2.5% analytical uncertainties on the ratio. Only magma residing longer than three centuries at depth will have measurably lower (^{226}Ra/^{230}Th) than the initial ratio. Moreover, only magma residing for less than 5 kyrs will have detectable ^{226}Ra excess over ^{230}Th, which is the case for historical dacite from Hekla volcano

Radium-thorium disequilibrium is very modest in historical Hekla products and absent in prehistoric pumice or lava. The highest ^{226}Ra excess over ^{230}Th (14%) is observed in the basalt and decreases to approximately 5% with magma differentiation (Table 1). Similar results were obtained by Chekol et al. (2011) on the Lambafit 1913 CE basalt and post-eighteenth century basaltic andesite—andesite lava from Hekla. Decreasing Ra–Th disequilibrium with magma differentiation has been observed world-wide and used to constrain magmatic timescales (Vigier et al. 1999; Condomines et al. 2003; Turner et al. 2003; Blake and Rogers 2005; Reagan et al. 2005; Cooper and Kent 2014).

The modest ^{226}Ra–^{230}Th disequilibrium in Hekla products puts a limit on its usefulness in discussing timescales given the analytical uncertainties (Fig. 5). Only magma residence times longer than 300 years and shorter than 5000 years will be accessible if the parental basalt had (^{226}Ra/^{230}Th) of only 1.16.

Discussion

^{226}Ra–^{230}Th disequilibria in Hekla products

Extracting timescale information from changing ^{226}Ra–^{230}Th disequilibria with magma differentiation is possible when the effect of magma differentiation on the decreasing Ra–Th disequilibrium can first be assessed. The well-known decline of (^{226}Ra/^{230}Th) with magma evolution is observed from Hekla basalt to basaltic andesite (from 1.15 to 1.04) after

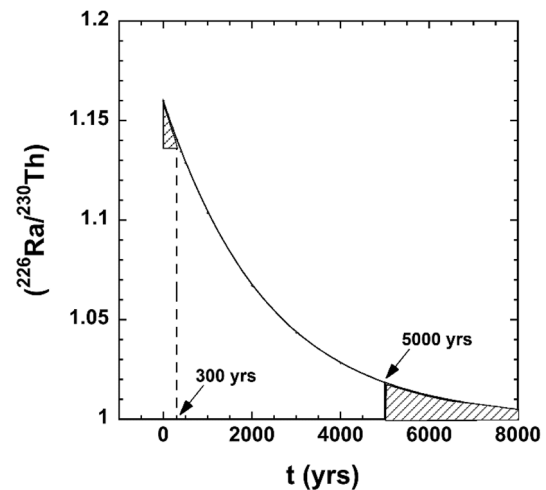which the disequilibrium remains uniform from basaltic andesite through andesite to dacite (approximately 5% Ra-excess over Th). If the uniform (^{226}Ra/^{230}Th) from magma of intermediate to silicic composition were to reflect fractional crystallisation then the bulk partition coefficients of both Ra and Th would have to be equal. However, apatite fractionation from magma of intermediate composition is expected to alter the Ra/Th (Kokfelt et al. 2009; Chekol et al. 2011). The weak ^{226}Ra-excess in the silicic magma more likely results from partial melting of the hydrated basaltic crust, upon which Mt. Hekla is built. Simple 10–15% batch melting of a basaltic crust in radioactive equilibrium can be shown to produce ^{226}Ra-excess within error of that measured in the Hekla dacite, if the bulk mineral-melt partition coefficients, D_{Ra} and D_{Th}, are close to nought and 0.01, respectively. The shortage of Ra partition coefficients and better knowledge of the accessory phases during crustal melting hamper firmer conclusions being drawn. The limited number of historical Hekla dacite also excludes detailed discussion of its ^{226}Ra–^{230}Th disequilibrium. Nevertheless, the small Ra–Th disequilibrium suggests that the dacite formed within the last 5 kyrs (Fig. 5).

Radium-thorium evolution during magma differentiation

Several studies have reached a consensus for the origin of basaltic andesite, the dominant historical magma type erupted at Hekla volcano. Approximately 50% fractional crystallisation (FC) from basaltic magma of composition

like that of the 1913 Lambafit basalt is the preferred mechanism. A mineral assemblage composed of plagioclase (An_{60}, 41%), augite (34%), FeTi-oxides (17%) and olivine (8%) fractionating from Hekla basalt forms basaltic icelandite melt (Sigmarsson et al. 1992). Apatite is an abundant accessory mineral in the more evolved magma (basaltic andesite, andesite, dacite and rhyolite; Sigvaldason 1974; Jakobsson 1979; Chekol et al. 2011; Geist et al. 2021; Sigmarsson et al. 2022). The effect of the FC differentiation mechanism from basalt to basaltic andesite on the Ra–Th disequilibrium is readily assessed from the Rayleigh fractionation law (Fig. 6).

The bulk Th partition coefficient (D_{Th}) between minerals and melt is calculated as 0.008 from measured D_{Th} between individual minerals and glass from Hekla products (Sigmarsson et al. 2022) and their proportions in the fractionating mineral assemblage. For a negligible D_{Th}, the slope of the linear regression of log $(^{226}Ra)_0$ vs. log Th concentrations is equal to $1 - D_{Ra}$, the bulk partition coefficient of Ra. From the slope of 0.90, a bulk partition coefficient of 0.10 is obtained between the fractionating mineral assembly and the derived melt. A bulk D of the same order of magnitude was obtained for alkaline basalt to hawaite–mugearite differentiation forming the magma suite of Vestmannaeyjar, south of Iceland (bulk $D_{Ra} = 0.25$; Sigmarsson 1996) and Etna basalt-hawaiite evolution (Condomines et al. 1995). The same slope from basaltic andesite to dacite in Fig. 6 is not in favour of a fractional crystallisation mechanism alone since a higher bulk partition coefficient for Th is expected during apatite fractionation in magma of intermediate to silicic composition (Kokfelt et al. 2009; Chekol et al. 2011).

A similar approach can be applied to the recent lava results by Chekol et al (2011) using a somewhat different formulation of the Rayleigh law (Condomines et al. 2005). In Fig. 7 are plotted the measured concentrations of
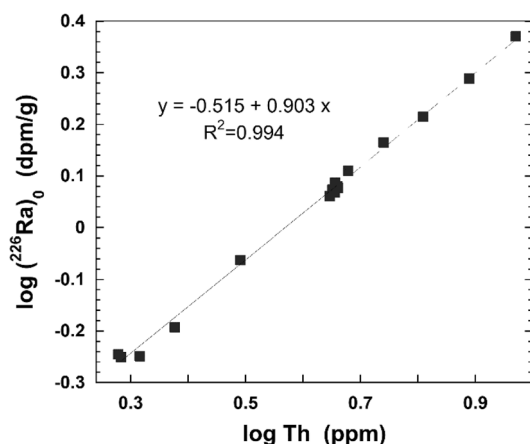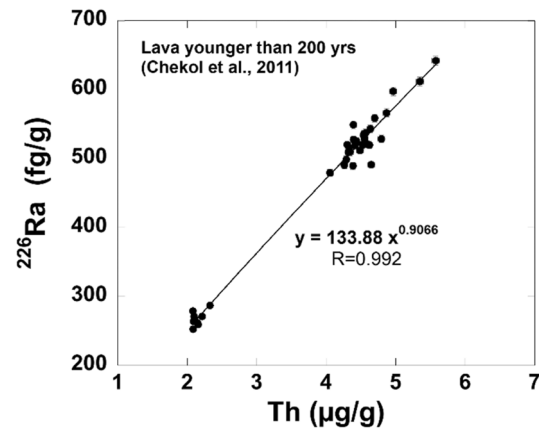
Fig. 7 Power regression of Ra vs. Th weight concentrations in Hekla lavas younger than 1845 CE (Chekol et al. 2011) revealing an exponent of 0.91 that yields a bulk Ra partition coefficient of 0.09 for a fractional crystallisation model

radium and thorium in lavas younger than two centuries, hence the measured ^{226}Ra is indistinguishable from the eruption value $^{226}Ra_0$. The fractionation law for Ra and Th is $^{226}Ra_0 = {}^{226}Ra_i\, f^{D_{Ra}-1}$ and $Th = Th_i\, f^{D_{Th}-1}$ where the subscript i denotes the parental magma concentrations, f the melt fraction and D the bulk Ra partition coefficient. Assuming $D_{Th} \sim 0$ and substituting Th/Th_i for f leads to

$$^{226}Ra_0 = {}^{226}Ra_i(Th/Th_i)^{1-D}$$

and from the correlation in Fig. 7, the D_{Ra} is calculated as 0.09. The variable Ra concentrations measured by Chekol et al. (2011) in the young lava of Hekla thus yield the same Ra partition coefficient as that derived from different Hekla lava and tephra of this study (Fig. 6).

Therefore, both studies yield a bulk D_{Ra} of 0.1 from which the plagioclase partition coefficient can be derived. Plagioclase is the only phase of the mineral fractionating assembly in the basalt capable of incorporating Ra (e.g., Blundy and Wood 2003). The D_{Ra} (plagioclase-melt) is therefore simply equal to 0.10/0.41, or 0.24. Very few experimental results on the Ra partition coefficient are available. Those of Fabrizzio et al. (2009) are shown for four feldspar compositions in Fig. 8. A linear interpolation between the result for An_{81} and An_{34}, yield D of 0.25 for a plagioclase of An_{56}, which is the predominant composition of plagioclase phenocrysts in the last four Hekla eruptions (Baldridge et al. 1973; Geist et al. 2021; Fig. 8 inset). Therefore, both the empirical approach using the Rayleigh law and the experimental results yield indistinguishable Ra partition coefficients between plagioclase and melt. The consequence is that all the Ra variability between basalt and basaltic andesite at Hekla is readily explained by fractional crystallisation alone.
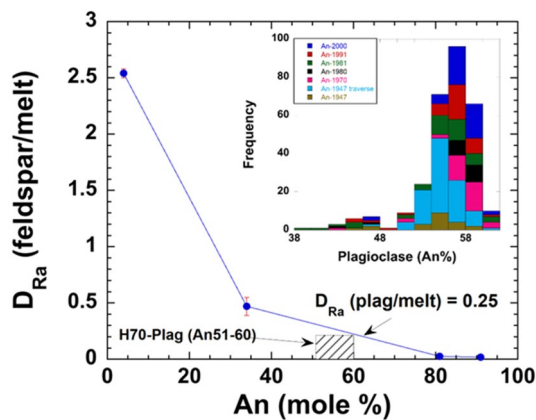
Fig. 6 The slope on a plot of log Ra vs. log Th is equal to $1 - D_{Ra}$, if D_{Th} is nought, during fractional crystallisation from basalt to basaltic andesite. The bulk Ra partition coefficient for Hekla is thus 0.1

Fig. 8 Experimental results on the Ra partition coefficient between feldspar and melt from Fabrizzio et al. (2009). The feldspar composition in twentieth century Hekla volcanics from Baldridge et al. (1973) and Geist et al. (2021) with a frequency top at An_{56-58}. Linear interpolation yields D_{Ra} of 0.25 between An_{56} plagioclase and melt. Inset: Plagioclase compositions in the last five Hekla eruptions (Geist et al. 2021; see Supplementary Material 1)

Estimating magma reservoir size

The fact that decreasing ($^{226}Ra/^{230}Th$) from basalt to the basaltic andesite at Hekla is fully explained by plagioclase fractionation, out of the steady-state melt produced at the end of Hekla eruptions, constrains the duration of basalt differentiation to be shorter than 300 years. The time span may well be shorter but cannot be precisely detected with the current analytical capabilities for Ra measurements (Fig. 5). The duration of magma differentiation must be shorter than the residence time of the basaltic andesite steady-state magma since all eruptions end with basaltic andesite of the same composition (rather than smaller ^{226}Ra-excess if differentiation time was longer). Consequently, the magma reservoir volume can be estimated from the measured flux at the surface and the maximum residence time (τ) of the magma. The magma flux (Q) in and out of a magma reservoir in a steady state is identical, and equal to its volume (V) divided by the residence time, or $Q_{in} = Q_{out} = V/\tau$. However, estimating Q relies on the approximation that the magma production rate observed at the surface represents the flux in and out of the magma chamber.

Seismicity before an eruption of Hekla is of a notoriously short duration (approximately 90 min; Soosalu et al. 2005) and migrates vertically to the surface during rapid magma ascent (approximately 8 m/s; Soosalu and Einarsson 2004). The magma leaving a reservoir at more than 10 km depth (Geirsson et al. 2012; Sturkell et al. 2013; Baxter et al. 2023) thus ascends to surface without arresting on the way. Consequently, the estimated magma productivity at surface should be close to the flux out (Q_{out}) of the basaltic andesite magma reservoir. In that case the volume of the basaltic andesite

magma reservoir can be estimated from the maximum residence time as $V < 0.0053$ km^3/years $\times 300$ years $= 1.6$ km^3. For a hypothetical spherical and a 10 km long pipe-shaped magma chamber (Geirsson et al. 2012) the radius would be <730 m and <400 m, respectively, which may be too small to be identified by seismic waves. Such a small size concurs with the suggested absence of a large magma chamber under Hekla from seismic waves (Soosalu and Einarsson 2004). From the results discussed above the best geochemical estimate of the volume of the basaltic andesite magma accumulation zone is in the range of 0.1–1.6 km^3.

Conclusion

The main results are the following:

- Linear correlation of Th concentration in the first emitted tephra of historical eruptions at Hekla volcano with the length of the foregoing quiescent period has been established. A similar correlation proposed for SiO_2 (Thorarinsson 1967) is thus confirmed.
- The intercept with the *Y*-axis at a repose time of nought yields Th of 4.4 ppm that is close to the average composition of the lavas erupted at the end of each eruption, representing the steady-state composition of the basaltic andesite magma accumulation zone at depth. Steady-state behaviour is verified from the cumulative magma volume versus time (Wadge 1982).
- Small ^{226}Ra excesses over its parent ^{230}Th in basaltic andesite are entirely explained by plagioclase fractionation during differentiation from basalt magma. No detectable ^{226}Ra-decay allows estimation of a maximum 300 years residence time.
- Linear correlations of lava production with the length of the foregoing quiescent period permits estimation of the magma flux, which multiplied by the maximum residence time, yields the basaltic andesite magma reservoir volume close to 2 km^3.

References

Baldridge SW, McGetchin TR, Frey FA (1973) Magmatic evolution of Hekla, Iceland. Contrib Mineral Petrol 42:245–258. https://doi.org/10.1007/BF00371589

Baxter RJM, Maclennan J, Neave DA, Thordarson T (2023) Depth of magma storage under Iceland controlled by magma fluxes. Geochem Geophys Geosystems 24:e2022GC010811. https://doi.org/10.1029/2022GC010811

Berlo K, Turner S, Blundy J, Hawkesworth C (2004) The extent of U-series disequilibria produced during partial melting of the lower crust with implications for the formation of the Mount St. Helens Dacites Contrib Mineral Petrol 148:122–130. https://doi.org/10.1007/s00410-004-0590-2

Blake S, Rogers N (2005) Magma differentiation rates from (^{226}Ra/^{230}Th) and the size and power output of magma chambers. Earth Planet Sci Lett 236:654–669. https://doi.org/10.1016/j.epsl.2005.05.035

Blundy JD, Wood BJ (2003) Mineral-melt partitioning of uranium, thorium and their daughters. Rev Mineral Geochem 52:59–118. https://doi.org/10.2113/0520059

Carpentier M, Gannoun A, Pin C, Sigmarsson O (2016) New thorium isotope ratio measurements in silicate reference materials: A-THO, AGV-2, BCR-2, BE-N, BHVO-2 and BIR-1. Geostand Geoanal Res 40:239–256. https://doi.org/10.1111/j.1751-908X.2015.00385.x

Chekol TA, Kobayashi K, Yokoyama T, Sakaguchi C, Nakamura E (2011) Timescales of magma differentiation from basalt to andesite beneath Hekla Volcano, Iceland: constraints from U-series disequilibria in lavas from the last quarter-millennium flows. Geochim Cosmochim Acta 75:256–283. https://doi.org/10.1016/j.gca.2010.10.001

Condomines M, Tanguy JC, Michaud V (1995) Magma dynamics at Mt. Etna: constraints from U-Th–Ra–Pb radioactive disequilibria and Sr isotopes in historical lavas. Earth Planet Sci Lett 132:25–41. https://doi.org/10.1016/0012-821X(95)00052-E

Condomines M, Gauthier P-J, Sigmarsson O (2003) Timescales of magma chamber processes and dating of young volcanic rocks. Rev Mineral Geochem 52:125–174. https://doi.org/10.2113/0520125

Condomines M, Gauthier PJ, Tanguy JC, Gertisser R, Thouret JC, Berthommier P, Camus G (2005) ^{226}Ra or ^{226}Ra/Ba dating of Holocene volcanic rocks: application to Mt. Etna and Merapi volcanoes. Earth Planet Sci Lett 230:289–300. https://doi.org/10.1016/j.epsl.2004.12.002

Cooper KM, Kent AJR (2014) Rapid remobilization of magmatic crystals kept in cold storage. Nature 506:480–483. https://doi.org/10.1038/nature12991

Costa F, Shea T, Ubide T (2020) Diffusion chronometry and the timescales of magmatic processes. Nat Rev Earth Environ 1:201–214. https://doi.org/10.1038/s43017-020-0038-x

Fabrizzio A, Schmidt MW, Günther D, Eikenberg J (2009) Experimental determination of Ra mineral/melt partitioning for feldspars and ^{226}Ra-disequilibrium crystallization ages of plagioclase and alkali-feldspar. Earth Planet Sci Lett 280:137–148. https://doi.org/10.1016/j.epsl.2009.01.022

Geirsson H, LaFemina P, Arnadottir Th, Sturkell E, Sigmundsson F, Travis M, Schmidt P, Lund B, Hreinsdottir S, Bennett R (2012) Volcano deformation at active plate boundaries: deep magma accumulation at Hekla volcano and plate boundary deformation in south Iceland. J Geophys Res Solid Earth. https://doi.org/10.1029/2012JB009400

Geist D, Harpp K, Oswald P, Wallace P, Bindeman I, Christensen B (2021) Hekla revisited: fractionation of a magma body at

historical timescales. J Petrol 62:egab001. https://doi.org/10.1093/petrology/egab001

Handley HK, Turner SP, Smith IEM, Stewart RB, Cronin SJ (2008) Rapid timescales of differentiation and evidence for crustal contamination at intra-oceanic arcs: geochemical and U-Th–Ra–Sr–Nd isotopic constraints from Lopevi Volcano, Vanuatu, SW Pacific. Earth Planet Sci Lett 273:184–194. https://doi.org/10.1016/j.epsl.2008.06.032

Holden NE (1990) Total half-lives for selected nuclides. Pure Appl Chem 62:941–958. https://doi.org/10.1351/pac199062050941

Jakobsson SP (1979) Petrology of recent basalts of the Eastern Volcanic Zone, Iceland. Acta Nat Isl 26:1–103

Kjartansson G (1945) Hekla. Árbók Ferðafélags Íslands (Yearbook of the Iceland Travel Association), Reykjavik, 155 pp

Kokfelt TF, Hoernle K, Lundstrom C, Hauff F, van den Bogaard C (2009) Time-scales for magmatic differentiation at the Snaefellsjökull central volcano, western Iceland: constraints from U-Th–Pa–Ra disequilibria. Geochim Cosmochim Acta 73:1120–1144. https://doi.org/10.1016/j.gca.2008.11.02

Larsen G, Thordarson Th (2016) Hekla. In: Oladottir B, Larsen G, Guðmundsson MT (eds) Catalogue of Icelandic volcanoes. IMO, UI and CPD-NCIP. https://icelandicvolcanos.is/?volcano=HEK. Retrieved 24 Nov 2023

Óladóttir BA, Larsen G, Sigmarsson O (2012) Deciphering eruption history and magmatic processes from tephra in Iceland. Jökull 62:21–38

Pedersen GBM, Belart JMC, Magnússon E, Vilmundardóttir OK, Kizel F, Sigurmundsson FS, Gísladóttir G, Benediktsson JA (2018a) Hekla Volcano, Iceland, in the 20th century: lava volumes, production rates, and effusion rates. Geophys Res Lett 45:1805–1813. https://doi.org/10.1002/2017GL076887

Pedersen GBM, Montalvo J, Einarsson P, Vilmundardóttir OK, Sigurmundsson FS, Belart JMC, Hjartardóttir ÁR, Kizel F, Rustowicz R, Falco N, Gísladóttir G, Benediktsson JA (2018b) Historical lava flow fields at Hekla volcano, South Iceland. Jökull 68:1–26. https://doi.org/10.33799/jokull2018.68.001

Pommé S, Jerome SM, Venchiarutti C (2014) Uncertainty propagation in nuclear forensics. Appl Radiat Isot 89:58–64. https://doi.org/10.1016/j.apradiso.2014.02.005

Porter C, Howat I, Noh MJ, Husby E, Khuvis S, Danish E, Tomko K, Gardiner J, Negrete A, Yadav B, Klassen J, Kelleher C, Cloutier M, Bakker J, Enos J, Arnold G, Bauer G, and Morin P (2023) ArcticDEM, Version 4.1, Harvard Dataverse, V1. https://doi.org/10.7910/DVN/3VDC4W. Accessed 12 June 2023.

Pyle DM (1992) The volume and residence time of magma beneath active volcanoes determined by decay-series disequilibria methods. Earth Planet Sci Lett 112:61–73. https://doi.org/10.1016/0012-821X(92)90007-I

Reagan MK, Tepley FJ III, Gill JB, Wortel M, Hartman B (2005) Rapid time scales of basalt to andesite differentiation at Anatahan volcano, Marian Islands. J Volcanol Geotherm Res 146:171–183. https://doi.org/10.1016/j.jvolgeores.2004.10.022

Schlieder TD, Cooper KM, Kent AJR, Bradshaw R, Huber C (2022) Thermal storage conditions and origin of compositional diversity of plagioclase crystals in magmas from the 1980 and 2004–2005 eruptions of Mount Saint Helens. J Petrol 63:1–34. https://doi.org/10.1093/petrology/egac064

Sigmarsson O (1996) Short magma chamber residence time at an Icelandic volcano inferred from U-series disequilibria. Nature 382:440–442. https://doi.org/10.1038/382440a0

Sigmarsson O, Condomines M, Fourcade S (1992) A detailed Th, Sr, and O isotope study of Hekla: differentiation processes in an Icelandic volcano. Contrib Mineral Petrol 112:20–34. https://doi.org/10.1007/BF00310953

Sigmarsson O, Bergþórsdóttir IA, Devidal J-L, Larsen G, Gannoun A (2022) Long or short silicic magma residence time beneath Hekla

volcano, Iceland? Contrib Mineral Petrol 177:13. https://doi.org/10.1007/s00410-021-01883-5

Sigvaldason GE (1974) The petrology of Hekla and origin of silicic rocks in Iceland. In the Eruption of Hekla 1947–1948. Soc Sci Islandica 5:1–44

Soosalu H, Einarsson P (2004) Seismic constraints on magma chambers at Hekla and Torfajökull volcanoes, Iceland. Bull Volcanol 66:276–286. https://doi.org/10.1007/s00445-005-0417-7

Soosalu H, Einarsson P, Thorbjarnardottir BS (2005) Seismic activity related to the 2000 eruption of the Hekla volcano, Iceland. Bull Volcanol 68:21–36

Sturkell E, Ágústsson K, Linde AT, Sacks SI, Einarsson P, Sigmundsson F, Geirsson H, Pedersen R, LaFemina PC, Ólafsson H (2013) New insights into volcanic activity from strain and other deformation data for the Hekla 2000 eruption. J Volcanol Geotherm Res 256:78–86. https://doi.org/10.1016/j.jvolgeores.2013.02.001

Thorarinsson S (1967) The eruptions of Hekla in historical times. In: Einarsson T, Kjartansson G, Thorarinsson S (eds) The eruption of Hekla 1947–1948. I. Societas Scientiarum Islandica, Reykjavík, pp 1–177

Turner S, Foden J, George R, Evans P, Varne R, Elburg M, Jenner G (2003) Rates and processes of potassic magma evolution beneath Sangeang Api Volcano, East Sunda Arc Indonesia. J Petrol 44:491–515. https://doi.org/10.1093/petrology/44.3.491

Vigier N, Bourdon B, Joron JL, Allègre CJ (1999) U-decay series and trace element systematics in the 1978 eruption of Ardoukoba, Asal rift: timescale of magma crystallization. Earth Planet Sci Lett 174:81–98. https://doi.org/10.1016/S0012-821X(99)00256-3

Wadge G (1982) Steady state volcanism: evidence from eruption histories of polygenetic volcanoes. J Geophys Res 87:4035–4049. https://doi.org/10.1029/JB087iB05p04035

Yokoyama T, Kuritani T, Kobayashi K, Nakamura E (2006) Geochemical evolution of a shallow magma plumbing system during the last 500 years, Miyakejima volcano, Japan: constraints from ^{238}U–^{230}Th–^{226}Ra systematics. Geochim Cosmochim Acta 70:2885–2901. https://doi.org/10.1016/j.gca.2006.02.027